

LETTER

Seasonal ecosystem metabolism across shallow benthic habitats measured by aquatic eddy covariance

Karl M. Attard ^{1,2*} Iván F. Rodil,^{1,3} Ronnie N. Glud,^{2,4} Peter Berg ⁵ Joanna Norkko,¹ Alf Norkko^{1,3}

¹Tvärminne Zoological Station, University of Helsinki, Hanko, Finland; ²Department of Biology, University of Southern Denmark, Odense M, Denmark; ³Baltic Sea Centre, Stockholm University, Stockholm, Sweden; ⁴Department of Ocean and Environmental Sciences, Tokyo University of Marine Science and Technology, Tokyo, Japan; ⁵Department of Environmental Sciences, University of Virginia, Charlottesville, Virginia

Scientific Significance Statement

Shallow seafloor (benthic) habitats are highly biodiverse and productive regions, but there remains considerable uncertainty in their contribution to coastal productivity. This has limited our understanding of the importance of nearshore biogenic habitats. Using aquatic eddy covariance, a recent technological development that can be applied to a wide range of habitats, this study investigates six key Baltic Sea habitats over a year spanning highly contrasting biogenic communities, from rocky algal canopies to soft-sediment deposits. These measurements document the dominant role of benthic habitats for metabolism in shallow waters, and identify understudied rocky substrates as metabolism hotspots in the coastal zone. Eddy covariance measurements can thus elucidate the role of the different habitats in carbon and nutrient cycling and sequestration within heterogeneous coastal seascapes.

Abstract

Shallow benthic habitats are hotspots for carbon cycling and energy flow, but metabolism (primary production and respiration) dynamics and habitat-specific differences remain poorly understood. We investigated daily, seasonal, and annual metabolism in six key benthic habitats in the Baltic Sea using ~2900 h of in situ aquatic eddy covariance oxygen flux measurements. Rocky substrates had the highest metabolism rates. Habitat-specific annual primary production per m² was in the order *Fucus vesiculosus* canopy > *Mytilus trossulus* reef > *Zostera marina* canopy > mixed macrophytes canopy > sands, whereas respiration was in the order *M. trossulus* > *F. vesiculosus* > *Z. marina* > mixed macrophytes > sands > aphotic sediments. Winter metabolism contributed 22–31% of annual rates. Spatial upscaling revealed that benthic habitats drive >90% of ecosystem metabolism in waters ≤5 m depth, highlighting their central role in carbon and nutrient cycling in shallow waters.

*Correspondence: karl.attard@biology.sdu.dk

Associate editor: Jack Middelburg

Author Contribution Statement: K.M.A., I.F.R., R.N.G., and A.N. formulated the research questions and designed the study approach. K.M.A., I.F.R., and A.N. conducted the fieldwork. K.M.A., P.B., and I.F.R. processed the data. K.M.A. wrote the manuscript with input from all authors.

Data Availability Statement: Data can be retrieved from the Dryad Digital Repository at <https://doi.org/10.5061/dryad.p0g4t96>.

Additional Supporting Information may be found in the online version of this article.

This is an open access article under the terms of the Creative Commons Attribution License, which permits use, distribution and reproduction in any medium, provided the original work is properly cited.

Land-ocean transition zones are biodiversity and productivity hotspots. In addition to phytoplankton production occurring in the water column, the submerged coastal landscapes are colonized by a mosaic of distinct communities of seafloor (benthic) vegetation that play a significant role in the oceanic C cycle (Duarte 2017). Large emergent canopies of seagrass and macroalgae, along with biofilms of less conspicuous microscopic algae (microphytobenthos), are estimated to cover a third of the world's continental shelf (Gattuso et al. 2006). Vegetated habitats can synthesize organic matter at remarkably high rates ($> 100 \text{ mmol C m}^{-2} \text{ h}^{-1}$) (Bordeyne et al. 2017), forming extensive canopies and globally significant C stocks (Fourqurean et al. 2012). On an annual basis, vegetated canopies typically generate a surplus of organic C production (net autotrophy), and a substantial proportion ($\sim 40\%$) of their fixed C can be exported (Duarte and Cebrián 1996), enhancing secondary production in terrestrial and aquatic realms through spatial subsidies (Polis et al. 1997).

The important role of shallow benthic habitats for C cycling and energy flow has been known for decades (Mann 1973; Smith 1981; MacIntyre et al. 1996), but we remain widely uninformed about how metabolism (primary productivity and respiration) varies across the coastal seafloor. Obtaining overall estimates of coastal productivity across multiple habitats that span highly contrasting biogenic communities, from rocky algal canopies to soft-sediment environments, has been challenging due to a lack of a common methodology allowing for comparable metabolism estimates. This has limited our understanding of the contribution of biogenic habitats to coastal productivity. Importantly, habitats with contrasting structural biodiversity elements may have very different productivity patterns, despite occurring in close proximity (Eyre and Maher 2011). The first step toward being able to understand productivity in heterogeneous coastal areas is therefore to perform comparative measures of metabolism across the mosaic of habitats that characterize the coastal seascape, and then to extend these measurements over the year to resolve their seasonal dynamics.

In this study, we explore benthic metabolism within the shallow eutrophic waters of the Baltic Sea. We investigate metabolism dynamics in six contrasting shallow subtidal habitats over a year, each representing a major habitat type of the nearshore Baltic (canopies of *Fucus vesiculosus*, *Zostera marina*, and mixed macrophytes, a *Mytilus trossulus* reef, photic sandy sediments, and a deeper aphotic muddy basin). We used the aquatic eddy covariance (AEC) oxygen flux method (Berg et al. 2003), a recent technological development that allows investigating habitat-scale (10s of m^2) metabolic rates and their drivers noninvasively at a high temporal resolution (1 h or less) (Berg et al. 2007; Berg et al. 2017). Based on this extensive data set, which also incorporates data on species' abundance and biomass, we elucidate the potential role of the different habitats in C and nutrient cycling, sequestration, and energy transfer within a highly heterogeneous coastal setting.

Materials and methods

Study location and sampling

Our six study sites were located nearby the Tvärminne Zoological Station on the Hanko Peninsula in SW Finland (59.844°N , 23.249°E), and consisted of five photic habitats and one deeper aphotic site (Fig. 1), namely: bare sediments (photic: 3 m depth, sandy sediment, and aphotic: 34 m depth, muddy sediment), a mixed macrophyte canopy (3 m depth, sandy), a seagrass canopy (*Z. marina*, 3.5 m depth, sandy), a macroalgal canopy (*F. vesiculosus*, 2.0 m depth, rocky), and a mussel reef (*M. trossulus*, 5 m depth, rocky). In total, flux measurements were performed on 40 occasions between May 2016 and December 2017.

Biological sampling

We developed a sampling protocol to quantify dominant features of seafloor biodiversity within the eddy covariance flux footprint (Rodil et al. 2019). The extracted samples were used to estimate the standing biomass (g C m^{-2}) of the main phototrophic components and macrofauna of each habitat using conversion ratios for dry weight (macrophytes), ash-free dry weight (macrofauna), or chlorophyll *a* (microphytobenthos) (Supporting Information Section S1).

Benthic oxygen fluxes

Benthic metabolism rates were computed from O_2 fluxes quantified in situ using the AEC technique (Berg et al. 2003). Our AEC systems have two fast-response O_2 microsensors ($T_{90} \leq 0.3 \text{ s}$, low stirring sensitivity $< 1\%$) (Revsbech 1989) for redundancy and comparison. These sensors are interfaced with an acoustic Doppler velocimeter (Nortek; Fig. 1f) (McGinnis et al. 2011). This setup is capable of resolving very small fluxes down to $1 \text{ mmol O}_2 \text{ m}^{-2} \text{ d}^{-1}$ or less by capturing the entire range of flux-contributing turbulent eddies under typical hydrodynamic conditions within the benthic boundary layer (Berg et al. 2009). Additional sensors located on the AEC frame logged transmitted (seabed) photosynthetically active radiation (PAR) (LI-192, Li-Cor), water temperature and salinity (U24 HOBO), and dissolved O_2 concentration (U26 HOBO) every 15 min.

We followed standard guidelines for instrument setup and data processing (Lorrai et al. 2010; Donis et al. 2015) (Supporting Information Section S2). Computing daily metabolism rates from the 15 min fluxes followed a three-step process (Fig. 2). For each deployment, multiple days of quality-checked O_2 fluxes and PAR were averaged by the time of day to produce a single continuous 24 h time series. The minimum number of flux days per deployment was 1.0, the maximum was 4.9, and the mean was 3.0 (Supporting Information Table S1). The fluxes were then separated into daytime fluxes (FLUX_{day} ; when $\text{PAR} > 0.0 \mu\text{mol m}^{-2} \text{ s}^{-1}$) and nighttime fluxes ($\text{FLUX}_{\text{night}}$; when $\text{PAR} < 0.0 \mu\text{mol m}^{-2} \text{ s}^{-1}$), and the PAR time series was used to determine the number of daylight hours (h_{day}). Daily gross primary productivity (GPP, $\text{mmol O}_2 \text{ m}^{-2} \text{ d}^{-1}$) was computed as $\text{GPP} = (\text{FLUX}_{\text{day}} + |\text{FLUX}_{\text{night}}|) * h_{\text{day}}$. Respiration rates (R , $\text{mmol O}_2 \text{ m}^{-2} \text{ d}^{-1}$) were calculated as $R = |\text{FLUX}_{\text{night}}| * 24$. Net

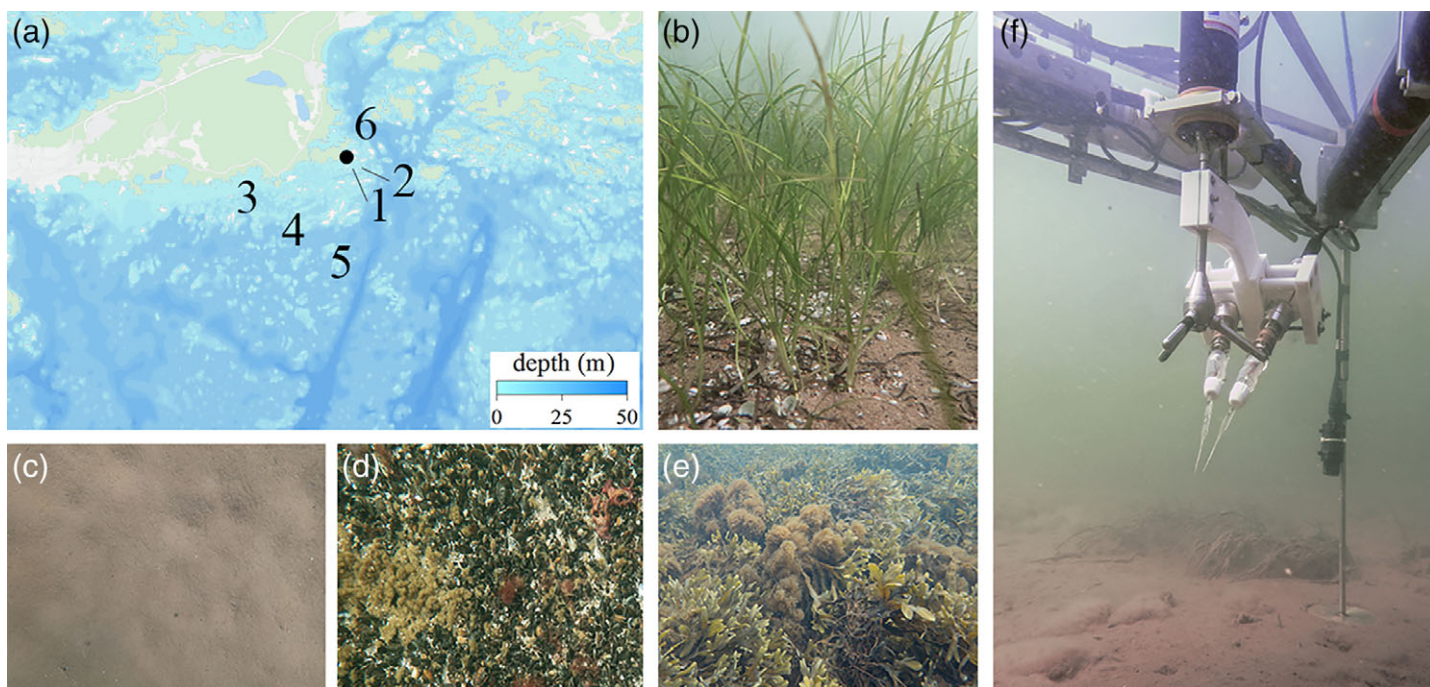


Fig. 1. Photos of equipment and study sites: **(a)** The location of the six study sites in SW Finland (1 = mixed macrophytes, 2 = bare sand, 3 = *Z. marina*, 4 = *F. vesiculosus*, 5 = *M. trossulus*, 6 = aphotic sediments, black dot = location of the Tvärminne Zoological Station), **(b)** the *Z. marina* canopy (height ~ 20 cm), **(c)** the bare sediments site (sand; frame size 40 * 30 cm), **(d)** the *M. trossulus* reef (shell size ~ 3 cm), **(e)** the *F. vesiculosus* canopy (height ~ 15 cm), and **(f)** the eddy covariance instrument (leg height = 80 cm).

ecosystem metabolism (NEM) was computed as the difference between daily GPP and R . Positive NEM indicates surplus organic C and O_2 production (autotrophy); negative NEM indicates net heterotrophy. Daily GPP, R , and NEM were converted to C equivalents ($g\ C\ m^{-2}\ d^{-1}$) assuming a quotient of 1.0 for both primary productivity and respiration. Annual rates were estimated as the numerical integration (mathematical area) of daily GPP, R , and NEM over Julian days using linear interpolation to gap-fill between discrete measurements. Linear regression was performed on the accumulated signals for GPP, R , and NEM over the year to investigate whether the slope of the integration was significantly different from zero (95% confidence level for fitting parameters). Numerical integration and statistical analyses were performed in OriginPro 2018 (OriginLab Corporation).

Results

Sampling sites

Bottom-water temperature ranged from 0.2°C in March to 16.5°C in August, and salinity was between 5.2 and 6.7 throughout the year. Daily PAR ranged from 0.4 $mol\ m^{-2}\ d^{-1}$ at the *Z. marina* site in December to 30.7 $mol\ m^{-2}\ d^{-1}$ at the *F. vesiculosus* canopy (shallowest site) in June (Supporting Information Table S1).

Biomass of plants and macrofauna

Plant biomass at the mixed macrophyte site and at the *Z. marina* canopy was dominated by the eelgrass *Z. marina*,

with occasional loose-lying accumulations of ephemeral, filamentous algae comprising up to 28% of total biomass. Total plant biomass ranged from 15 to 28 $g\ C\ m^{-2}$ at the mixed macrophyte site (6–50% below-ground) and from 15 to 43 $g\ C\ m^{-2}$ at the *Z. marina* canopy (8–25% below-ground). Photosynthetic biomass at the *F. vesiculosus* canopy was an order of magnitude higher, ranging from 195 to 396 $g\ C\ m^{-2}$, with ephemeral macroalgae comprising <3%.

Macrofauna biomass generally was similar at the sand, deep mud, mixed macrophyte, and *F. vesiculosus* sites (annual range from 2 to 10 $g\ C\ m^{-2}$). The *Z. marina* canopy had slightly higher macrofauna biomass within the range of 6–14 $g\ C\ m^{-2}$, while the mussel reef had the highest macrofauna biomass of the five shallow sites, with values ranging seasonally from 21 to 34 $g\ C\ m^{-2}$.

Benthic metabolism measurements

The flux data set we present consists of 2926 h of benthic fluxes. Individual data sets used to calculate daily metabolism rates ranged from 24 to 117 h in duration (average = 73 h) (Supporting Information Table S1).

The highest daily rates of GPP were measured at the *F. vesiculosus* site in June (2.4 $g\ C\ m^{-2}\ d^{-1}$), coinciding with highest seabed PAR up to 1350 $\mu mol\ m^{-2}\ s^{-1}$ and the longest photic period ($h_{day} = 20\ h$). Daily R was highest at the mussel site in August (1.8 $g\ C\ m^{-2}\ d^{-1}$), coinciding with the warmest water temperatures for the year at this site of 15°C. Daily NEM ranged from strongly net heterotrophic at the mussel

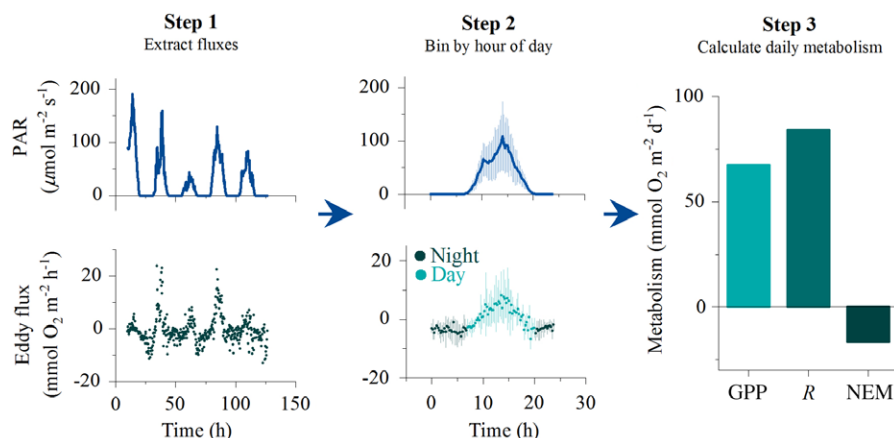


Fig. 2. General framework for computing daily seafloor metabolism rates from eddy covariance oxygen fluxes. Example data set is from the mussel reef in March. Error bars in step 2 are ± 1 SD.

site in August ($-1.0 \text{ g C m}^{-2} \text{ d}^{-1}$) to strongly net autotrophic at the *F. vesiculosus* site in June ($2.0 \text{ g C m}^{-2} \text{ d}^{-1}$) (Supporting Information Table S1).

In early winter (December), benthic metabolism rates were low at the five photic habitats, with daily GPP ranging from 0.1 to 0.2 $\text{g C m}^{-2} \text{ d}^{-1}$, and daily NEM ranging from net heterotrophic to metabolic balance (-0.2 to $0.0 \text{ g C m}^{-2} \text{ d}^{-1}$). However, in late winter (March), under colder water temperatures and higher light availability, we measured substantially higher rates of daily GPP at all five photic habitats (0.2 – $1.1 \text{ g C m}^{-2} \text{ d}^{-1}$). Altogether, winter GPP (1st December to 31st March) accounted for a significant proportion of annual GPP: 28% at the *Z. marina* site, 22% at *F. vesiculosus* canopy, 30% at mussel bed, 29% at the bare sediments site, and 26% at the mixed macrophytes site. Winter was similarly important for habitat R, accounting for between 27% and 31% of annual R at the shallow sites (Supporting Information Section S3).

The regression analysis that was performed on the annual integrated rates of GPP, R, and NEM indicated that in all but two cases, the slope differed significantly from zero at the 95% confidence level (R^2 value range from 0.45 to 1.0; global mean $R^2=0.94$). Annual NEM at the *Z. marina* site and at the sand site was not significantly different from zero ($R^2=-0.10$ and -0.16).

Annual GPP was highest at the *F. vesiculosus* site ($0.44 \text{ kg C m}^{-2} \text{ yr}^{-1}$). Surprisingly, the mussel reef showed remarkably high rates of GPP ($0.17 \text{ kg C m}^{-2} \text{ yr}^{-1}$) that were comparable in magnitude to those that were measured at the *Z. marina* canopy ($0.16 \text{ kg C m}^{-2} \text{ yr}^{-1}$; Fig. 3). The mixed macrophyte canopy and the sand site had a similar annual GPP (0.10 and $0.07 \text{ kg C m}^{-2} \text{ yr}^{-1}$). Annual R was lowest at the aphotic muddy site ($0.04 \text{ kg C m}^{-2} \text{ yr}^{-1}$) and highest at the mussel site ($0.35 \text{ kg C m}^{-2} \text{ yr}^{-1}$). Despite being located at greater depth, the aphotic site had surprisingly high annual R rates, comparable to those measured at some shallower sites (Fig. 3, Supporting Information Table S1). The *F. vesiculosus* canopy was strongly net autotrophic on an annual basis ($\text{NEM}=0.29 \text{ kg C m}^{-2} \text{ yr}^{-1}$), whereas

the mussel reef, despite a high annual GPP, was strongly net heterotrophic ($\text{NEM}=-0.18 \text{ kg C m}^{-2} \text{ yr}^{-1}$). The mixed macrophyte canopy had a low annual NEM of $0.01 \text{ kg C m}^{-2} \text{ yr}^{-1}$, while annual NEM at the *Z. marina* site and the sand site were not significantly different from zero. The aphotic site had an annual NEM of $-0.04 \text{ kg C m}^{-2} \text{ yr}^{-1}$ (Fig. 3).

Discussion

Seasonal benthic metabolism

Obtaining daily estimates of coastal productivity across multiple habitats that span highly contrasting biogenic communities has been challenging due to a lack of a common methodology allowing for comparable metabolism measurements. For this reason, soft-sediment habitats have been the focus of numerous studies, whereas measurements in rocky substrates have not been performed with the same intensity, despite these habitats being largely characteristic of coastal areas in temperate and high-latitude regions. Importantly, rocky habitats can harbor a massive biomass of autotrophs such as large canopies of macroalgae, or heterotrophs such as dense bivalve reefs. The AEC approach makes it possible to compare these contrasting habitats.

In our study, the hard-bottom substrates represented the two “extremes” in benthic metabolism. The *F. vesiculosus* canopy was the most autotrophic habitat we investigated, and the mussel bed the most heterotrophic. The metabolism results from the hard-bottom substrates are perhaps also the most intriguing. Whereas high annual GPP at the *F. vesiculosus* site can be expected due to high autotrophic biomass, with values comparing well with existing GPP estimates for macroalgal canopies worldwide (Krause-Jensen and Duarte 2016), the high annual GPP at the mussel bed was surprising, given the greater depth of this habitat (lower light availability) and the small standing stock of autotrophic biomass, which consisted of biofilms and short tufts of ephemeral filamentous algae (Fig. 1d).

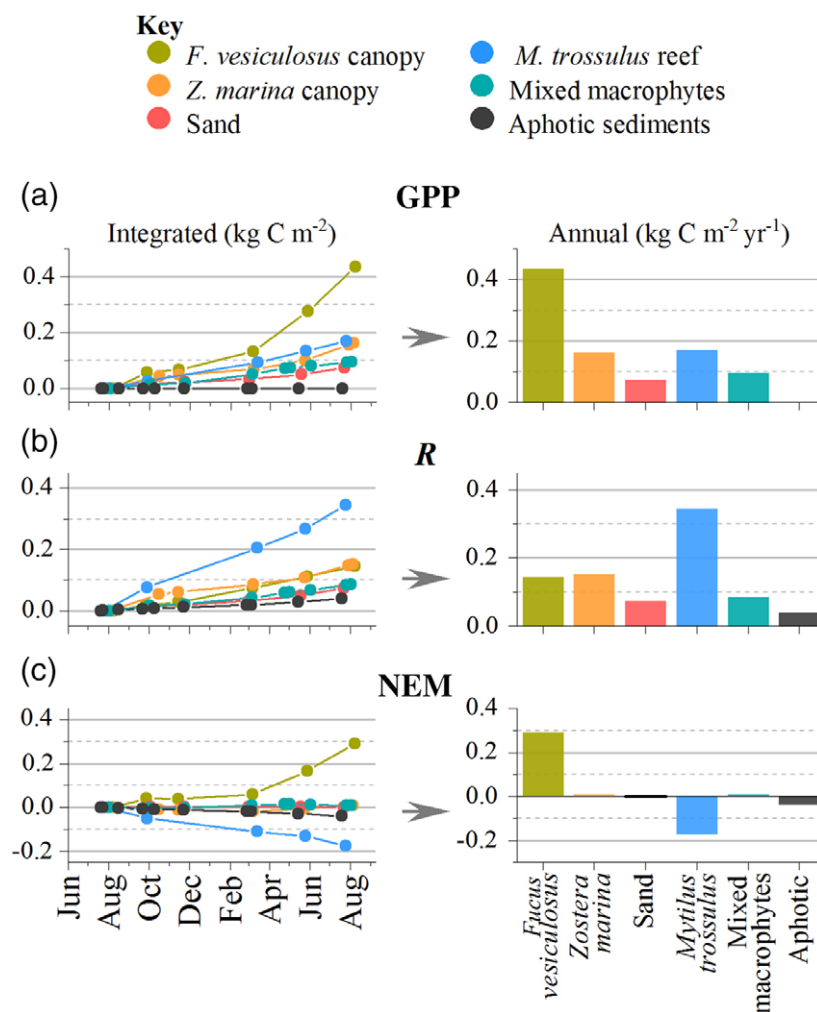


Fig. 3. Seasonal and annual seafloor gross primary production (GPP, **a**), respiration (R , **b**), and NEM (**c**) rates for the six investigated habitats. Annual NEM from the *Z. marina* canopy and the sand site is not significantly different from zero. Rate values can be found in Supporting Information Table S1.

The high annual GPP at the mussel bed, which amounted to almost half of that at the *F. vesiculosus* site, and was comparable to that measured at the *Z. marina* canopy, suggests efficient recycling of nutrients and C between heterotrophs and autotrophs in the absence of other substantial sources of regenerated nutrients such as sediment deposits. Filter-feeding bivalves such as mussels may play a similar important role in nutrient regeneration through active filtration, deposition of feces and pseudo-feces, and efficient exchange of nutrient-rich waters near the seabed (Kautsky and Evans 1987; Nishizaki and Ackerman 2017). These processes may be important in maintaining high benthic GPP, thereby providing a significant autochthonous organic matter subsidy that was equivalent to ~50% of the annual R rate of the mussel reef habitat in our case. Similar direct positive effects between suspension-feeding bivalves and benthic primary producers have been observed in tide-pool communities (Pfister 2007), and remarkably high primary production rates have also been reported for intertidal oyster beds (Volaric et al. 2018).

Despite being net heterotrophic, shallow-water bivalve reefs may synthesize large amounts of organic matter that may significantly offset their annual C demand. Due to the underlying rocky substrate, it is expected that the synthesized autotrophic biomass is either consumed by the mussels, and thus recycled within the habitat itself, or it is exported to surrounding depositional environments along with detrital pools originating from other shallow habitats such as *F. vesiculosus* beds (Attard et al. 2019). At the deeper aphotic site, the annual benthic C demand of the depositional basin sediments ($0.04 \text{ kg C m}^{-2} \text{ yr}^{-1}$) was comparable to the annual water column NEM ($0.05 \text{ kg C m}^{-2} \text{ yr}^{-1}$ for the 10 m depth photic zone) (Kuparinen et al. 1984). When considering that this site has an estimated annual C burial rate of ~50% (data not shown), these results suggest significant connectivity with external sources of organic C likely originating from shallower depths (e.g., export from shallow photic habitats) or from inland waters.

The onset of winter in shallow, high-temperature benthic habitats is often characterized by overwintering of fauna in deeper

waters and burrows, and suppressed biotic interactions and energy flows (Möller et al. 1985). Our measurements of benthic metabolism in early and late winter show contrasting results. Whereas low rates of metabolism ($GPP \leq 0.2 \text{ g C m}^{-2} \text{ d}^{-1}$) are evident in December, with habitats largely being net heterotrophic (up to $-0.2 \text{ g C m}^{-2} \text{ d}^{-1}$), late winter (March) GPP is mostly above $0.2 \text{ g C m}^{-2} \text{ d}^{-1}$ and as high as $1.1 \text{ g C m}^{-2} \text{ d}^{-1}$ at the *F. vesiculosus* site. Some habitats were strongly net autotrophic during this period (NEM up to $0.6 \text{ g C m}^{-2} \text{ d}^{-1}$). Despite cold water temperature of $1\text{--}2^\circ\text{C}$, the benthic habitats were able to photosynthesize efficiently. It is likely that sufficient light and ample nutrients in late winter following a largely heterotrophic autumn and early winter period make conditions favorable for photosynthetic production, resulting in large amounts of C being produced during winter, up to a third of annual benthic GPP. Similar observations have been made for other high-temperate and Arctic settings (Attard et al. 2014), although measurements of benthic metabolism in winter still remain scarce.

Spatial upscaling

The importance of individual habitats to coastal GPP, R , and NEM was estimated by upscaling our annual measurements to habitat distribution models (20 m grid resolution) that are available for our study area (Virtanen et al. 2018) (Fig. 4). To do this, we defined a 93 km^2 area encompassing all of our study site locations, and limited our analyses to shallow photic depths (0–5 m; 13 km^2), where most of the benthic photosynthetic biomass is located (Virtanen

et al. 2018). Habitat distribution models for these shallow depths indicate a dominance of *F. vesiculosus* ($5.1 \text{ km}^2 \approx 40\%$ habitat coverage), followed by bare seabed ($4.4 \text{ km}^2 \approx 34\%$ coverage), *M. trossulus* ($1.8 \text{ km}^2 \approx 14\%$ coverage), and *Z. marina* ($1.6 \text{ km}^2 \approx 13\%$ coverage). Pelagic estimates are from literature values that are available for the study area ($GPP = 0.17 \text{ kg C m}^{-2} \text{ yr}^{-1}$, $R = 0.12 \text{ kg C m}^{-2} \text{ yr}^{-1}$, $NEM = 0.05 \text{ kg C m}^{-2} \text{ yr}^{-1}$) (Kuparinen et al. 1984; Lignell 1990; Raateoja et al. 2004), and have been scaled linearly to water depth. Using this approach, we identify a remarkably large contribution of benthic habitats for metabolism in shallow waters: the seafloor was responsible for 93% of annual ecosystem GPP, 92% of ecosystem R , and 95% of the ecosystem's surplus autochthonous C production (NEM), which was dominated by the highly autotrophic *F. vesiculosus* canopies (Fig. 4) (Attard et al. 2019). Furthermore, *F. vesiculosus* mediates around two-thirds of the total ecosystem GPP in shallow waters, and *M. trossulus* reefs appear to be of similar importance to *Z. marina* canopies for GPP in our study area. Benthic habitats are therefore hotspots of production in shallow waters. In the Baltic Sea, broad-scale estimates of benthic GPP are largely based upon microalgal production, with rates of $\sim 0.1\text{--}0.3 \text{ g C m}^{-2} \text{ d}^{-1}$ in summer (Ask et al. 2016). From our measurements, it is evident that shallow benthic habitats, and complex habitats in particular (*Z. marina*, *M. trossulus*, *F. vesiculosus*), can mediate areal rates of GPP that are an order of magnitude higher than these current estimates. Incorporating the contributions of complex benthic habitats into broad-scale estimates of coastal productivity is therefore important.

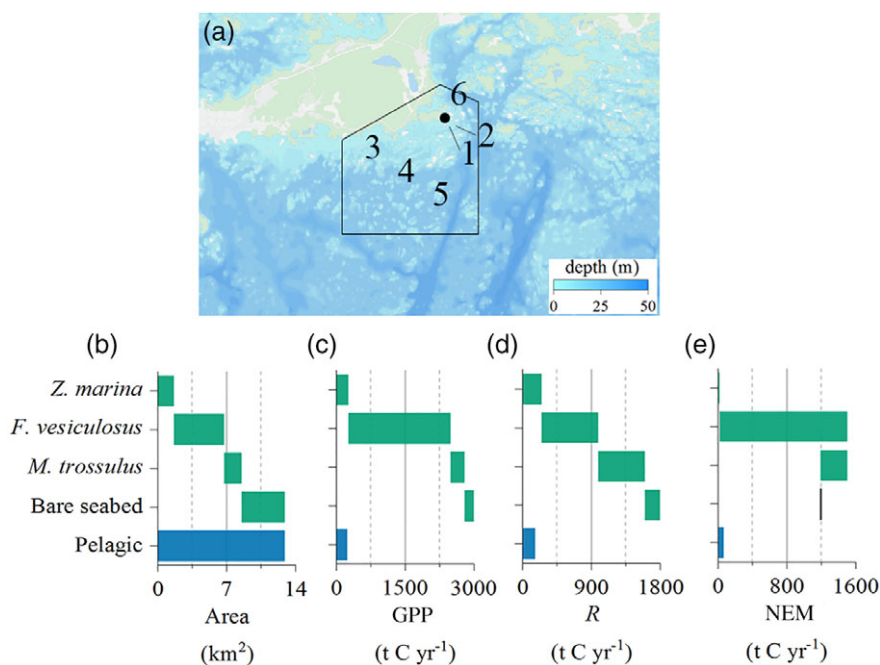


Fig. 4. Spatial upscaling of annual metabolism rates to a 93 km^2 habitat map that is available for *Z. marina*, *F. vesiculosus*, and *M. trossulus* in the study area, considering only shallow photic depths (0–5 m; 13 km^2). The solid line on the map in (a) delineates the area considered, and the black dot marks the location of the Tvärminne Zoological Station. Numbers indicate location of the six study sites. Habitat coverage (b) was combined with areal metabolism rates to estimate gross primary production (GPP, c), respiration (R , d) and net ecosystem metabolism (NEM, e). Pelagic estimates are from literature values (see “Discussion” section) and have been scaled linearly to water depth. GPP and R values are positive whereas NEM can be positive or negative.

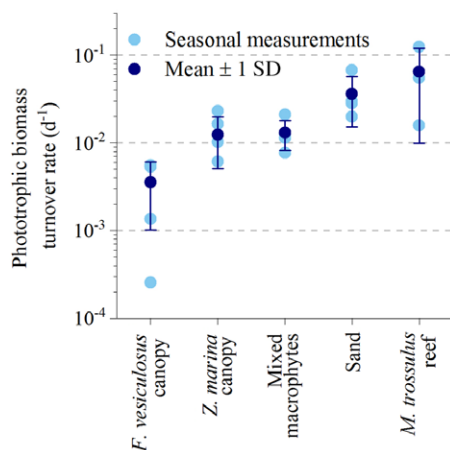


Fig. 5. Phototrophic C turnover rates for the different photic habitats, estimated as the ratio between daily GPP ($\text{g C m}^{-2} \text{ d}^{-1}$) and standing stock of autotrophic biomass (g C m^{-2}).

Biomass turnover rates

Partitioning of biomass production between different phototrophic components within each habitat (e.g., macrophytes, epiphytic microalgae) has important implications for food-web ecology and biogeochemical cycling (Sand-Jensen and Borum 1991; McGlathery et al. 2007). AEC fluxes quantify habitat-scale metabolism that include contributions from all phototrophic components. By considering the ratio between daily benthic GPP ($\text{g C m}^{-2} \text{ d}^{-1}$) and the estimated standing phototrophic biomass (B , g C m^{-2}), we can infer the phototrophic C turnover rates (d^{-1}) for different phototrophic habitats and seasons (Fig. 5). Using this analysis, we deduce that habitats with low phototrophic biomass consisting primarily of microalgae and thin ephemeral macroalgae (bare sediments, mussel bed) have rapid phototrophic biomass turnover rates ($\sim 0.07 \text{ d}^{-1}$), whereas large perennial canopies such as *F. vesiculosus* turn over their biomass on much longer time-scales ($\sim 0.003 \text{ d}^{-1}$). These results are consistent with the notion that newly produced biomass from microalgae and ephemeral macroalgae is rapidly grazed and decomposed (Sand-Jensen and Borum 1991; Duarte and Cebrián 1996), whereas large perennial macrophytes grow slower (e.g., 0.03 d^{-1} for *F. vesiculosus* during the main growth period) (Sand-Jensen and Borum 1991), but they attain much larger standing biomass, providing habitat structure and contributing to storage of atmospheric CO_2 (Fourqurean et al. 2012; Krause-Jensen and Duarte 2016). Over the past century, perennial macrophyte canopies have deteriorated in the Baltic Sea due to eutrophication, favoring instead the proliferation of vast underwater fields of ephemeral macroalgae (Kautsky et al. 1986; Boström et al. 2003). This shift in the structural habitat biodiversity promotes low standing phototrophic biomass, rapid C and nutrient turnover, and potential for a larger local secondary production, at the cost of reducing overall canopy habitat structure and the C and nutrient sequestration capacity of the coastal zone (McGlathery et al. 2007).

References

- Ask, J., O. Rowe, S. Brugel, M. Stromgren, P. Bystrom, and A. Andersson. 2016. Importance of coastal primary production in the northern Baltic Sea. *Ambio* **45**: 635–648. doi:[10.1007/s13280-016-0778-5](https://doi.org/10.1007/s13280-016-0778-5)
- Attard, K. M., R. N. Glud, D. F. McGinnis, and S. Rysgaard. 2014. Seasonal rates of benthic primary production in a Greenland fjord measured by aquatic eddy correlation. *Limnol. Oceanogr.* **59**: 1555–1569. doi:[10.4319/lo.2014.59.5.1555](https://doi.org/10.4319/lo.2014.59.5.1555)
- Attard, K. M., I. F. Rodil, P. Berg, J. Norkko, A. Norkko, and R. N. Glud. 2019. Seasonal metabolism and carbon export potential of a key coastal habitat: The perennial canopy-forming macroalga *Fucus vesiculosus*. *Limnol. Oceanogr.* **64**: 149–164. doi:[10.1002/lno.11026](https://doi.org/10.1002/lno.11026)
- Berg, P., and others. 2003. Oxygen uptake by aquatic sediments measured with a novel non-invasive eddy-correlation technique. *Mar. Ecol. Prog. Ser.* **261**: 75–83. doi:[10.3354/meps261075](https://doi.org/10.3354/meps261075)
- Berg, P., H. Røy, and P. L. Wiberg. 2007. Eddy correlation flux measurements: The sediment surface area that contributes to the flux. *Limnol. Oceanogr.* **52**: 1672–1684. doi:[10.4319/lo.2007.52.4.1672](https://doi.org/10.4319/lo.2007.52.4.1672)
- Berg, P., and others. 2009. Eddy correlation measurements of oxygen uptake in deep ocean sediments. *Limnol. Oceanogr.: Methods* **7**: 576–584. doi:[10.4319/lom.2009.7.576](https://doi.org/10.4319/lom.2009.7.576)
- Berg, P., M. L. Delgard, R. N. Glud, M. Huettel, C. E. Reimers, and M. L. Pace. 2017. Non-invasive flux measurements at the benthic interface: The aquatic eddy covariance technique. *Limnol. Oceanogr. e-Lect.* **7**: 1–50. doi:[10.1002/loe2.10005](https://doi.org/10.1002/loe2.10005)
- Bordeyne, F., A. Migne, and D. Davoult. 2017. Variation of fucoid community metabolism during the tidal cycle: Insights from *in situ* measurements of seasonal carbon fluxes during emersion and immersion. *Limnol. Oceanogr.* **62**: 2418–2430. doi:[10.1002/lno.10574](https://doi.org/10.1002/lno.10574)
- Boström, C., S. P. Baden, and D. Krause-Jensen. 2003. The seagrasses of Scandinavia and the Baltic Sea, p. 27–37. In E. P. Green and F. T. Short [eds.], *World atlas of seagrasses*. Univ. of California Press.
- Donis, D., and others. 2015. An assessment of the precision and confidence of aquatic eddy correlation measurements. *J. Atmos. Ocean. Technol.* **32**: 642–655. doi:[10.1175/JTECH-D-14-00089.1](https://doi.org/10.1175/JTECH-D-14-00089.1)
- Duarte, C. M. 2017. Reviews and syntheses: Hidden forests, the role of vegetated coastal habitats in the ocean carbon budget. *Biogeosciences* **14**: 301–310. doi:[10.5194/bg-14-301-2017](https://doi.org/10.5194/bg-14-301-2017)
- Duarte, C. M., and J. Cebrián. 1996. The fate of marine autotrophic production. *Limnol. Oceanogr.* **41**: 1758–1766. doi:[10.4319/lo.1996.41.8.1758](https://doi.org/10.4319/lo.1996.41.8.1758)
- Eyre, B. D., and D. Maher. 2011. Mapping ecosystem processes and function across shallow seascapes. *Cont. Shelf Res.* **31**: S162–S172. doi:[10.1016/j.csr.2010.01.013](https://doi.org/10.1016/j.csr.2010.01.013)
- Fourqurean, J. W., and others. 2012. Seagrass ecosystems as a globally significant carbon stock. *Nat. Geosci.* **5**: 505–509. doi:[10.1038/ngeo1477](https://doi.org/10.1038/ngeo1477)

- Gattuso, J. P., B. Gentili, C. M. Duarte, J. A. Kleypas, J. J. Middelburg, and D. Antoine. 2006. Light availability in the coastal ocean: Impact on the distribution of benthic photosynthetic organisms and their contribution to primary production. *Biogeosciences* **3**: 489–513. doi:[10.5194/bg-3-489-2006](https://doi.org/10.5194/bg-3-489-2006)
- Kautsky, N., H. Kautsky, U. Kautsky, and M. Waern. 1986. Decreased depth penetration of *Fucus vesiculosus* (L) since the 1940s indicates eutrophication of the Baltic Sea. *Mar. Ecol. Prog. Ser.* **28**: 1–8. doi:[10.3354/meps028001](https://doi.org/10.3354/meps028001)
- Kautsky, N., and S. Evans. 1987. Role of biodeposition by *Mytilus-edulis* in the circulation of matter and nutrients in a Baltic coastal ecosystem. *Mar. Ecol. Prog. Ser.* **38**: 201–212. doi:[10.3354/meps038201](https://doi.org/10.3354/meps038201)
- Krause-Jensen, D., and C. M. Duarte. 2016. Substantial role of macroalgae in marine carbon sequestration. *Nat. Geosci.* **9**: 737–742. doi:[10.1038/ngeo2790](https://doi.org/10.1038/ngeo2790)
- Kuparinen, J., J. M. Leppanen, J. Sarvala, A. Sundberg, and A. Virtanen. 1984. Production and utilization of organic matter in a Baltic ecosystem off Tvärminne, southwest coast of Finland. *Rapp. P.-V. Reun. Cons. Int. Explor. Mer.* **183**: 180–192.
- Lignell, R. 1990. Excretion of organic-carbon by phytoplankton - its relation to algal biomass, primary productivity and bacterial secondary productivity in the Baltic Sea. *Mar. Ecol. Prog. Ser.* **68**: 85–99. doi:[10.3354/meps068085](https://doi.org/10.3354/meps068085)
- Lorrai, C., D. F. McGinnis, P. Berg, A. Brand, and A. Wüest. 2010. Application of oxygen eddy correlation in aquatic systems. *J. Atmos. Ocean. Technol.* **27**: 1533–1546. doi:[10.1175/2010JTECHO723.1](https://doi.org/10.1175/2010JTECHO723.1)
- MacIntyre, H. L., R. J. Geider, and D. C. Miller. 1996. Microphytobenthos: The ecological role of the “secret garden” of unvegetated, shallow-water marine habitats. 1. Distribution, abundance and primary production. *Estuaries* **19**: 186–201. doi:[10.2307/1352224](https://doi.org/10.2307/1352224)
- Mann, K. H. 1973. Seaweeds - their productivity and strategy for growth. *Science* **182**: 975–981. doi:[10.1126/science.182.4116.975](https://doi.org/10.1126/science.182.4116.975)
- McGinnis, D. F., and others. 2011. Simple, robust eddy correlation amplifier for aquatic dissolved oxygen and hydrogen sulfide flux measurements. *Limnol. Oceanogr.: Methods* **9**: 340–347. doi:[10.4319/lom.2011.9.340](https://doi.org/10.4319/lom.2011.9.340)
- McGlathery, K. J., K. Sundback, and I. C. Anderson. 2007. Eutrophication in shallow coastal bays and lagoons: The role of plants in the coastal filter. *Mar. Ecol. Prog. Ser.* **348**: 1–18. doi:[10.3354/meps07132](https://doi.org/10.3354/meps07132)
- Möller, P., L. Pihl, and R. Rosenberg. 1985. Benthic faunal energy-flow and biological interaction in some shallow marine soft bottom habitats. *Mar. Ecol. Prog. Ser.* **27**: 109–121. doi:[10.3354/meps027109](https://doi.org/10.3354/meps027109)
- Nishizaki, M., and J. D. Ackerman. 2017. Mussels blow rings: Jet behavior affects local mixing. *Limnol. Oceanogr.* **62**: 125–136. doi:[10.1002/lno.10380](https://doi.org/10.1002/lno.10380)
- Pfister, C. A. 2007. Intertidal invertebrates locally enhance primary production. *Ecology* **88**: 1647–1653. doi:[10.1890/06-1913.1](https://doi.org/10.1890/06-1913.1)
- Polis, G. A., W. B. Anderson, and R. D. Holt. 1997. Toward an integration of landscape and food web ecology: The dynamics of spatially subsidized food webs. *Annu. Rev. Ecol. Syst.* **28**: 289–316. doi:[10.1146/annurev.ecolsys.28.1.289](https://doi.org/10.1146/annurev.ecolsys.28.1.289)
- Raateoja, M., J. Seppala, and H. Kuosa. 2004. Bio-optical modeling of primary production in the SW Finnish coastal zone, Baltic Sea: Fast repetition rate fluorometry in Case 2 waters. *Mar. Ecol. Prog. Ser.* **267**: 9–26. doi:[10.3354/meps267009](https://doi.org/10.3354/meps267009)
- Revsbech, N. P. 1989. An oxygen microsensor with a guard cathode. *Limnol. Oceanogr.* **34**: 474–478. doi:[10.4319/lno.1989.34.2.0474](https://doi.org/10.4319/lno.1989.34.2.0474)
- Rodil, I. F., K. M. Attard, J. Norkko, R. N. Glud, and A. Norkko. 2019. Towards a sampling design for characterizing habitat-specific benthic biodiversity related to oxygen flux dynamics using aquatic eddy covariance. *PLoS One* **14**: e0211673. doi:[10.1371/journal.pone.0211673](https://doi.org/10.1371/journal.pone.0211673)
- Sand-Jensen, K., and J. Borum. 1991. Interactions among phytoplankton, periphyton, and macrophytes in temperate fresh-waters and estuaries. *Aquat. Bot.* **41**: 137–175. doi:[10.1016/0304-3770\(91\)90042-4](https://doi.org/10.1016/0304-3770(91)90042-4)
- Smith, S. V. 1981. Marine macrophytes as a global carbon sink. *Science* **211**: 838–840. doi:[10.1126/science.211.4484.838](https://doi.org/10.1126/science.211.4484.838)
- Virtanen, E. A., M. Viitasalo, J. Lappalainen, and A. Moilanen. 2018. Evaluation, gap analysis, and potential expansion of the Finnish marine protected area network. *Front. Mar. Sci.* **5**: 402. doi:[10.3389/fmars.2018.00402](https://doi.org/10.3389/fmars.2018.00402)
- Volaric, M. P., P. Berg, and M. A. Reidenbach. 2018. Oxygen metabolism of intertidal oyster reefs measured by aquatic eddy covariance. *Mar. Ecol. Prog. Ser.* **599**: 75–91. doi:[10.3354/meps12627](https://doi.org/10.3354/meps12627)

Acknowledgments

We are grateful to our colleagues at the Tvärminne Zoological Station for their help with fieldwork and logistics, and to Anni Glud at the University of Southern Denmark, who constructed the oxygen microsensors used in this study. Elina Virtanen at the Finnish Environmental Institute (SYKE) provided the spatial data used in the upscaling exercises. The bathymetric map is from The Finnish Inventory Programme for the Underwater Marine Environment (VELMU). The Walter and Andrée de Nottbeck Foundation supported this work through a postdoctoral fellowship to KMA and through a senior research fellowship to RNG. Further funding for this project was provided by research grants from The Academy of Finland (project ID 294853), the University of Helsinki and Stockholm University strategic fund for collaborative research (the Baltic Bridge initiative), Denmark’s Independent Research Fund (project ID 7014-00078), the European Commission through HADES-ERC (project ID 669947) and ATLAS (project ID 678760), and from the US National Science Foundation (OCE-1061364, OCE-1334848). This study has utilized research infrastructure facilities provided by FINMARI (Finnish Marine Research Infrastructure network, The Academy of Finland, project ID 283417). This output reflects only the authors’ views. The European Union and other funding bodies cannot be held responsible for any use that may be made of the information contained herein.

Submitted 20 November 2018

Revised 12 March 2019

Accepted 21 March 2019